

# Root Cause Analysis of Outliers with Missing Structural Knowledge

Nastaran Okati<sup>\*1</sup>, Sergio Hernan Garrido Mejia<sup>2</sup>, William Roy Orchard<sup>3</sup>,  
Patrick Blöbaum<sup>4</sup>, and Dominik Janzing<sup>4</sup>

<sup>1</sup>Max Planck Institute for Software Systems

<sup>2</sup>Max Planck Institute for Intelligent Systems

<sup>3</sup>University of Cambridge

<sup>4</sup>Amazon Research

## Abstract

Recent work conceptualized root cause analysis (RCA) of anomalies via quantitative contribution analysis using causal counterfactuals in structural causal models (SCMs). The framework comes with three practical challenges: (1) it requires the causal directed acyclic graph (DAG), together with an SCM, (2) it is statistically ill-posed since it probes regression models in regions of low probability density, (3) it relies on Shapley values which are computationally expensive to find.

In this paper, we propose simplified, efficient methods of root cause analysis when the task is to identify a unique root cause instead of quantitative contribution analysis. Our proposed methods run in linear order of SCM nodes and they require only the causal DAG without counterfactuals. Furthermore, for those use cases where the causal DAG is unknown, we justify the heuristic of identifying root causes as the variables with the highest anomaly score. To this end, we prove that anomalies with small scores are unlikely to cause those with large scores and show upper bounds for the likelihood of causal pathways with non-monotonic anomaly scores.

## 1 Introduction

Detecting anomalies in a large number of variables has become a huge effort in science and business application, ranging from meteorology [1], monitoring medical health [2, 3], monitoring of industrial fabrication [4], fraud detection [5], credit scoring [6], cloud applications [7, 8, 9, 10, 11, 12] and more [13, 14, 15, 16, 17]. Oftentimes it is not only important to detect the anomalies but also to answer the question of *why* the anomaly was observed, or in other words, find its *root cause*. This is important as it provides insight on how to mitigate the issue manifested in the anomaly, and is hence more actionable. A series of previous works use statistical correlations between features to explain the anomalous value in the target variable [18, 19, 20, 21, 22]. The major drawback with such approaches is that correlations between the anomalous variables and the target variable do not necessarily imply causation. Hence, recent works conceptualized RCA using a causal framework [23, 10, 24, 25, 26]. From a causal perspective, finding *causal* relations between anomalies that are simultaneously or consecutively observed in different variables is an important step in identifying the root cause, i.e., answering the question of which anomaly caused the other.

**Related work** We can categorize the related work into two groups: 1) those that require the causal DAG to find the root cause, and, 2) those which do not require the causal DAG or try to infer it from data. Considering the first lines of work, our work builds on [23] in terms of the definition of root cause, where the

---

\*Correspondence to: nastaran@mpi-sws.org

authors use a causal graphical model based framework and utilize Shapley values to quantify the contribution of each of the variables to the extremeness of the target variable. [27, 28, 9] use a traversal-based approach that identifies a node as a root cause under two conditions: 1) none of its parent nodes exhibits anomalous behavior and 2) it is linked to the anomalous target node through a path of anomalous nodes. [29] apply such a traversal algorithm to data from cloud computing to find the root cause of performance drops in dependent services [12, 30, 31].

The main idea behind the second line of work is that if the DAG is unknown, the outliers themselves can support causal discovery.<sup>1</sup> In a scenario where several data points are available from the anomalous state (which we do not assume here), finding the root cause can also be modeled as the problem of identifying the intervention target of a soft intervention [34]. Likewise, [35, 36] describe how to use heavy-tailed distributions to infer the causal DAG for linear models. In a sense, this also amounts to using outliers for causal discovery – if one counts points in the tail as outliers.

**Our contributions** This paper tries to mitigate the practical challenges of RCA under the assumption that the task is restricted to identifying a *unique root cause* whose contribution dominates contributions of the other nodes, rather than quantitative contribution analysis. To this end, we relax the assumptions on the available causal information step by step: In Section 2, we first explain that interventional probabilities are sufficient and we do not need to rely on structural equation based counterfactuals.<sup>2</sup> This finding enables us to design the Topologically Ordered Contribution Analysis (TOCA) algorithm, presented in Section 3. In Section 4 we discuss how to avoid the statistical problem of estimating interventional probabilities and propose SMOOTH TRAVERSAL, an algorithm that inputs only the causal graph, and SCORE ORDERING, an algorithm that is only based on the ordering of the anomaly scores and hence, does not even need the causal graph. All our methods avoid a combinatorial explosion of terms in Shapley value based RCA. Section 5 compares the approaches on simulated and real-world data. The results suggest that the simplifications do not heavily impact the ability to find unique root causes.

## 2 Formal Framework for Root Cause Analysis

We first sketch the causal framework that our method and analysis are based on [38, 37]. Consider a system of  $n$  random variables  $(X_1, \dots, X_n) := \mathbf{X}$  and an underlying DAG corresponding to the causal relations between them in a way that a directed edge from  $X_i$  to  $X_j$  indicates that  $X_i$  directly causes  $X_j$ . Furthermore, we are given an SCM with structural equations

$$X_i := f_i(Pa_i, N_i), \quad (1)$$

which indicates that each variable  $X_i$  is a function of its parents  $Pa_i$  together with a noise variable  $N_i$ , where  $(N_1, \dots, N_n) := \mathbf{N}$  are jointly independent. We always assume  $X_n$  to be the sink node and the target of interest, whose anomaly is supposed to be explained via root causes further upstream. An iterative use of Eq. 1 results in a representation

$$X_n = F(N_1, \dots, N_n), \quad (2)$$

in which the structural causal information is implicit in the function  $F$ .

Consider the case where the value  $x_n$  of the target variable  $X_n$  is flagged as an outlier, and we wish to find the *unique root cause* of this outlier among the variables  $(X_1, \dots, X_n)$ . By Eq. 2 we have that  $x_n = F(n_1, \dots, n_n)$  where  $(n_1, \dots, n_n) := \mathbf{n}$  denote the corresponding values of the noise variables (which can be reconstructed from  $(x_1, \dots, x_n)$  for the class of invertible SCMs). This representation allows us to consider the contribution of each variable  $X_i$  to the outlier value in  $x_n$  in the target variable as the contribution of its noise term [23, 39].<sup>34</sup> The idea of attributing anomalies to noise terms is justified by the perspective that

<sup>1</sup>Note that this is aligned with the research direction of employing distributional changes for causal discovery [32, 33].

<sup>2</sup>rung 2 vs rung 3 in the ladder of causation [37])

<sup>3</sup>Throughout the paper, we assume the SCM is invertible and one can recover such noise values from the observed value of the variable together with that of its parents [40].

<sup>4</sup>Note that in [39] no algorithm for root cause analysis is proposed.

each  $n_j$  switches between deterministic mechanisms  $f_j(\cdot, n_j)$ , *response functions* [41], and the goal of RCA is to identify the *corrupted mechanisms* which did not work as usual, *i.e.*, the values  $x_j$  that do not follow the SCM  $x_j = f_j(Pa_j, n_j)$  with a value  $n_j$  in a "normal range". In other words, the recursive formulation allows us to attribute the extremeness in  $x_n$  to a corrupted noise term at one of the upstream nodes. As a result, the framework is based on the intuition that if  $X_j$  is the unique root cause, replacing  $n_j$  with a *normal* value would change  $x_n$  to a non-outlier, with high probability.

## 2.1 Anomaly Score

We next define an outlier score which we use in the next sections for our method and analysis. Let  $\tau : \mathcal{X} \rightarrow \mathbb{R}$  be an appropriate feature map which can be any existing outlier score function, mapping elements of  $\mathcal{X}$  to real values, for example, z-score.<sup>5</sup> Further, define the event

$$E := \{\tau(X_n) \geq \tau(x_n)\}, \quad (3)$$

of being at least as extreme as the observed event  $x_n$  according to the feature function  $\tau$ . From the point of view of statistical testing,  $\tau$  can be seen as test statistics for the null hypothesis that  $x_n$  is drawn from  $P(X_n)$ , *i.e.*,  $H_0 : x_n \sim P(X_n)$ , and  $P(\tau(X_n) \geq \tau(x_n)) = P(E)$  is the corresponding p-value. Note that small  $P(E)$  indicates that the null hypothesis is rejected with high confidence<sup>6</sup> and we rather assume that the usual mechanism generating samples from  $P(X_n)$  has been corrupted for that specific statistical unit. Since small p-values correspond to strong anomalies, we define the anomaly score by

$$S(x_n) = -\log P(\tau(X_n) \geq \tau(x_n)) = -\log P(E). \quad (4)$$

Since the logarithm of the probability of an event measures its *surprise* in information theory [13, 15], as in [23], we call anomaly scores with the above calibration *IT scores* for *information theoretic*. Given  $k$  observations  $x_n^1, \dots, x_n^k$  from  $P(X_n)$ , we will use the following simple estimator

$$\hat{S}(x_n^j) := -\log \frac{1}{k} |\{i \neq j \mid \text{with } \tau(x_n^i) \geq \tau(x_n^j)\}|. \quad (5)$$

It is important to note that this value can be at most  $\log k$ , *i.e.*, the estimated score can attain the value  $s$  only when at least  $e^s$  samples have been used.

## 2.2 Contribution Analysis

To compute the contribution of each noise  $N_i$  to the anomaly score of the outlier  $x_n$ , [23] measures how replacing the observed value  $n_i$  (originating from a potentially corrupted mechanism) with a normal value, changes the likelihood of the outlier event. Intuitively, this shows us the extent to which  $n_i$  has been responsible for the extremeness of  $x_n$ . This change of probability, however, should be measured given different contexts, with each context being the set of variables that are already changed to a normal value. To formalize this, for any subset of the index set,  $\mathcal{S} \subseteq \mathcal{U} := \{1, \dots, n\}$ , first note that the probability of the outlier event when all nodes in  $\mathcal{S}$  are set to their observed value and all the nodes in  $\bar{\mathcal{S}} = \mathcal{U} \setminus \mathcal{S}$  are randomized is  $P(E \mid \mathbf{N}_{\mathcal{S}} = \mathbf{n}_{\mathcal{S}})$ . Now the contribution of a node  $j \notin \mathcal{S}$  given the context  $\mathcal{S}$  is defined as:<sup>7</sup>

$$C(j \mid \mathcal{S}) := \log \frac{P(E \mid \mathbf{N}_{\mathcal{S}} = \mathbf{n}_{\mathcal{S}}, \mathbf{N}_j = \mathbf{n}_j)}{P(E \mid \mathbf{N}_{\mathcal{S}} = \mathbf{n}_{\mathcal{S}})}. \quad (6)$$

Let  $\Pi : \mathcal{U} \rightarrow \mathcal{U}$  be the set of all possible permutations of the nodes and  $\pi \in \Pi$  be any permutation. One then defines the contribution of a node  $j$  given permutation  $\pi$  as  $C^\pi(j) := C(j \mid I^{\pi < j})$ , where  $I^{\pi < j}$  denotes the set

<sup>5</sup>The z-score of a sample  $x$  is  $z = \frac{x - \mu}{\sigma}$  with  $\mu$  and *sigma* being the population mean, standard deviation respectively.

<sup>6</sup>This interpretation is certainly invalid in a standard anomaly *detection* scenario where Eq. 3 is repeatedly computed for every observation in a sequence. However, so-called anytime p-values [42] are outside of our scope.

<sup>7</sup>Note the difference in the definition of  $C(\cdot \mid \mathcal{S})$  compared to [23]. In our case  $\mathcal{S}$  is the set for which  $\mathbf{N}_{\mathcal{S}} = \mathbf{n}_{\mathcal{S}}$  while in [23]  $\mathbf{N}_{\mathcal{U} \setminus \mathcal{S}} = \mathbf{n}_{\mathcal{U} \setminus \mathcal{S}}$ .

of nodes that appear *before*  $j$  with respect to  $\pi$ , *i.e.*,  $I^{\pi < j} = \{i \in \mathcal{U} \mid \pi_i < \pi_j\}$ . We easily see that for each permutation  $\pi$ ,  $S(x_n)$  decomposes into the contributions of each node, *i.e.*,  $S(x_n) = \sum_{j \in \{1, \dots, n\}} C^\pi(j)$ . To symmetrize over all the possible permutations in  $\Pi$ , the Shapley contribution is calculated as:

$$C^{Sh}(j) := \frac{1}{n!} \sum_{\pi \in \Pi} C(j \mid I^{\pi < j}), \quad (7)$$

which is certainly expensive to compute [23]. Here, however, motivated by the fact that in most real-world scenarios there is a single corrupted factor causing anomalies, we try to find the *unique* node  $j$  with a corrupted mechanism, or the *unique root cause* of the outlier  $x_n$ . Our main assumption is that it is unlikely that nodes other than  $j$  get a significant value for their contribution. Note that this directly allows us to identify the root cause without the need for quantitatively finding the contribution of each and every node in the outlier value of the target variable  $X_n$ , which saves us exponential computations. In addition to the computational load, the symmetrization suffers from a more fundamental issue, namely that for most permutations  $\pi$ , the contributions  $C^\pi(j)$  rely on structural equations (rung 3 causal information according to the ladder of causation in [37]), while some  $C^\pi(\cdot)$  rely only on interventional probabilities, which can be computed from the graphical model (rung 2), which we explain in the next sub-section.

### 2.3 Interventional vs Counterfactual RCA

Since the SCM cannot be inferred from observational and interventional data, relying on the SCM is a serious bottleneck for RCA. Fortunately, as long as  $\pi$  is a topological ordering of nodes, no term in Eq. 7 requires the SCM. We explain this through an example for the bivariate causal relation  $X_1 \rightarrow X_2$ : given the SCM  $X_2 = f(X_1, N_2)$  and  $X_1 = N_1$ , randomizing  $N_2$  and fixing  $N_1 = n_1 = x_1$  generates  $X_2$  according to the observational conditional  $P(X_2 \mid x_1)$  (which no longer relies on the SCM), while, randomizing  $N_1$  and adjusting  $N_2 = n_2$  cannot be resolved into any observational term (see also Section 5 in [43]).<sup>8</sup> The following result generalizes this insight:

**Proposition 2.1** *Whenever  $\pi$  is a topological order of the causal DAG, *i.e.*, there are no arrows  $X_i \rightarrow X_j$  for  $\pi(i) > \pi(j)$ , all contributions  $C^\pi(j)$  can be computed from observational conditional distributions.*

All proofs can be found in Appendix B. This insight helps us design our first algorithm in the next section.

## 3 Simplified contribution analysis without counterfactuals

While we can never exclude the case where several mechanisms are corrupted, we always start with the working hypothesis that there has been only one. If this does not work, we can still try out hypotheses with more than one, but with the strong inductive bias of preferring explanations where most mechanisms worked as expected, in agreement with the so-called ‘sparse mechanism shift hypothesis’ in [44, 45].

Throughout this section, we assume without loss of generality that the indices  $X_1 \dots, X_n$  are topologically ordered with respect to the causal graph. We first describe the idea of our TOCA (Topologically Ordered Contribution Analysis) algorithm. We call this the oracle version of TOCA since we assume that the conditional probabilities are known:

1. For each  $i = 1, \dots, n$  compute  $P(E \mid n_1, \dots, n_i)$ . Since the variables are causally ordered, we have

$$P(E \mid n_1, \dots, n_i) = P(E \mid do(x_1), \dots, do(x_i)) = P(E \mid x_1, \dots, x_i).$$

Thus,  $P(E \mid n_1, \dots, n_i)$  can be inferred from *any* structural equation model that correctly reproduces the observed conditional probabilities.

---

<sup>8</sup>This can be checked by an SCM with two binaries where  $X_2 = X_1 \oplus N_2$ , with unbiased  $N_2$ , which induces the same distribution as the SCM  $X_2 = N_2$ , where  $X_1$  and  $X_2$  are disconnected and thus  $X_1$  does not get any contribution.

2. Infer the root cause  $j$  to be the index which maximizes the 'logarithmic probability gap'

$$C(i|\{1, \dots, i-1\}) = \log P(E|n_1, \dots, n_i) - \log P(E|n_1, \dots, n_{i-1}).$$

Although the size of the contribution depends on the order chosen, we will below state conditions under which it gets maximal for the unique root cause. To this end, we first generalize the notion of the contribution of a *single node* to the contribution of a *set*  $\mathcal{R} \subseteq \mathcal{U} \setminus \mathcal{S}$  of nodes, given the context  $\mathcal{S}$ , *i.e.*,

$$C(\mathcal{R}|\mathcal{S}) := \log \frac{P(E|\mathbf{N}_{\mathcal{R}} = \mathbf{n}_{\mathcal{R}}, \mathbf{N}_{\mathcal{S}} = \mathbf{n}_{\mathcal{S}})}{P(E|\mathbf{N}_{\mathcal{S}} = \mathbf{n}_{\mathcal{S}})}. \quad (8)$$

This notion becomes rather intuitive after observing that it is given by the sum of the contributions of all the elements in  $\mathcal{R}$  when they are one by one added to the context  $\mathcal{S}$ :

**Lemma 3.1** *For any set  $\mathcal{R} \subseteq \mathcal{U} \setminus \mathcal{S}$ , it holds that  $C(\mathcal{R}|\mathcal{S}) := C(j_1|\mathcal{S}) + \sum_{i=2}^k C(j_i|\mathcal{S} \cup \{j_1, \dots, j_{i-1}\})$  with  $\mathcal{R} = \{j_1, \dots, j_k\}$ .*

Next, the following result shows that it is unlikely to obtain high contributions when the noise values are randomly drawn from their usual distributions, *i.e.*, we have the following proposition:

**Proposition 3.2** *Whenever all noise variable in some set  $\mathcal{R}$  are sampled from  $P(\mathbf{N}_{\mathcal{R}})$ , it holds that  $P(C(\mathcal{R}|\mathcal{S}) \geq \alpha) \leq e^{-\alpha}$ .*

Note that the proposition allows that the variables  $N_j$  *not* in  $\mathcal{R}$  are drawn from a different distribution. Thus, Proposition 3.2 states that it is unlikely that a set that only contains *non-corrupted nodes* has high contribution.

**Definition 3.3 (dominating root cause)** *Node  $j$  is the dominating root cause with respect to the permutation  $\pi$  if we have for all  $i \in I^{\pi < j}$*

$$(i) \quad C(I^{\pi < i}|\emptyset) < S(x_n)/4,$$

*and further, for all  $i \in I^{\pi > j}$ , we have*

$$(ii) \quad C(I^{\pi > i}|I^{\pi \leq i}) < S(x_n)/4.$$

Due to Proposition 3.2, the assumptions of Definition 3.3 are met with probability at least  $1 - (n-1) \cdot e^{-\frac{1}{4}S(x_n)}$  using union bound. We then obtain:

**Theorem 3.4** *if the conditions of Definition 3.3 are met, the oracle version of TOCA finds the correct root cause  $j$ , since we have that :*

$$P(E|n_1, \dots, n_i) \begin{cases} \leq e^{-\frac{3}{4}S(x_n)} & \forall i < j \\ \geq e^{-\frac{1}{4}S(x_n)} & \forall i \geq j \end{cases} .$$

*Therefore, log probabilities jump by at least  $S(x_n)/2$  **only** for  $i = j$ .*

Appendix A contains the pseudocode for TOCA 1, provides a thorough discussion on the its key properties A.1, and discusses its sample complexity A.2 for estimating the contributions subject to the assumption that the given graphical model correctly reproduces conditional probabilities. Since inferring conditional probabilities is hard, we only recommend TOCA for the rare cases where the conditional probabilities are given, and now describe approaches to root cause analysis that avoid them. We have explained TOCA mainly because the following will heavily build upon its ideas, without suffering from the same statistical difficulties.

## 4 Contribution analysis when conditional probability estimation can be ill-posed

We have discussed methods that do not require SCMs and require only the graphical model, that is, the causal DAG endowed with observational conditional probabilities  $P(X_j|Pa_j)$ . However, inferring the latter is statistically ill-posed, particularly when the number of parents is large. While the additive noise assumption reduces the problem essentially to the regression problem of estimating conditional expectations, the problem remains ill-posed because analyzing outliers amounts to probing the regression models in regions with low density. Here we describe approaches that infer causal relations between anomalies from a given causal DAG together with marginal anomaly scores  $S(x_j)$ , using the simple estimator in Eq. 5. To this end, we start with the toy example of cause-effect pairs and then generalize it to more than two variables.

### 4.1 Outliers of Cause and Effect Pairs

Let the causal DAG be  $X \rightarrow Y$  for two variables  $X, Y$ , where we observe anomalies with anomaly scores  $S(x), S(y)$  that occur together. We argue now that merely the comparison of  $S(x)$  and  $S(y)$  provides some hints on whether mechanisms  $P(X)$  or  $P(Y|X)$  corrupted or both. To this end, we state the following assumptions:

1. **Monotonicity:** increasing the anomaly score of  $X$  does not decrease the probability of an anomaly event at  $Y$ :

$$P\{S(Y) \geq S(y)|S(X) = S(x)\} \leq P\{S(Y) \geq S(y)|S(X) \geq S(x)\}, \quad (9)$$

2. **Injectivity:** the mapping  $x \mapsto S(x)$  is one-to-one. This is the case, for instance, for scores obtained from *one-sided* tail probabilities, that is for  $\tau(x) := x$ .

We then define two different null hypotheses stating that the mechanisms  $P(X)$  or  $P(Y|X)$ , respectively, worked as usual:  $H_0^X$ :  $x$  has been drawn from  $P(X)$ , and  $H_0^Y$ :  $y$  has been drawn from  $P(Y|X = x)$  (where  $P(X, Y)$  denotes the joint distribution of  $X, Y$  in the normal mode). Note that  $H_0^Y$  allows that  $X$  is drawn from an arbitrary distribution instead of  $P(X)$ , only the mechanism generating  $y$  from  $x$  has remained the same. We then have the following criteria for rejecting  $H_0^X$  and  $H_0^Y$ :

**Lemma 4.1**  $H_0^X$  can be rejected at level  $p \leq e^{-S(x)}$ .

This follows immediately from the definition of IT scores in Eq. 4. On the other hand, we obtain:

**Lemma 4.2** Subject to Monotonicity and Injectivity assumptions,  $H_0^Y$  can be rejected at level  $p \leq e^{-|S(y)-S(x)|_+}$ , where  $|\cdot|_+$  denotes the positive part.

**Proof** Injectivity and monotonicity implies

$$P\{S(Y) \geq S(y)|X = x\} = P\{S(Y) \geq S(y)|S(X) = S(x)\} \leq P\{S(Y) \geq S(y)|S(X) \geq S(x)\}.$$

Since  $P(A|B) \leq P(A)/P(B)$  for any two events  $A, B$  the last term is at most  $\frac{P\{S(Y) \geq S(y)\}}{P\{S(X) \geq S(x)\}} = \frac{e^{-S(y)}}{e^{-S(x)}}$ . In a nutshell, Lemma 4.2 states that an anomaly of strength  $S(x)$  causes an anomaly of strength  $S(y)$  only with probability at most  $e^{-|S(y)-S(x)|_+}$ .

There is also a third alternative, namely that  $x$  and  $y$  are causally unrelated. Even if there is a causal connection between  $X$  and  $Y$ , for instance,  $X \rightarrow Y$ , it could happen that  $x$  being anomalous has been irrelevant for the anomaly  $y$  because  $P(Y|X = x) = P(Y)$ . In other words, although  $x$  is anomalous, it happens to be an anomaly that does not render an anomaly of  $Y$  more likely. The corresponding hypothesis  $H_0^{XY}$  reads that  $x$  has been drawn from  $P_X$  and  $y$  from  $P_Y$ . We find:

**Lemma 4.3**  $H_0^{XY}$  can be rejected at level  $p \leq e^{-S(x)-S(y)}[1 + S(x) + S(y)]$ .

The lemma follows from the fact that for independent variables  $X, Y$ , the corrected sum  $S(x) + S(y) - \log[1 + S(x) + S(y)] =: \tilde{S}((x, y))$  is a valid IT score for pairs and thus satisfies  $P\{\tilde{S}((X, Y)) \geq \tilde{S}((x, y))\} \leq e^{-\tilde{S}((x, y))}$ , see Theorem 1 in the arxiv version of [23].

Lemma 4.1 to 4.3 entail interesting consequences for the case where the causal direction is not known: Let  $S(x) = 10, S(y) = 5$ . For  $X \rightarrow Y$  we can only reject  $H_0^X$ , while mechanism  $P(Y|X)$  possibly worked as expected. However, for  $Y \rightarrow X$ , we would reject both hypotheses, that  $P(Y)$  and that  $P(X|Y)$  worked as expected with p-value  $e^{-5}$  each. Following the working hypothesis that at most one mechanism was corrupted we thus prefer  $X \rightarrow Y$ . Note that the third alternative of causally independent generation of  $x$  and  $y$  can be rejected even at level  $p \leq e^{-5-10}(1 + 5 + 10)$ .

**Connection to contribution analysis** calculations similar to the proof of Lemma 4.3 show that the contribution of  $y$  given  $x$  to the anomaly  $y$  is at least  $|S(y) - S(x)|_+$ , (while the contribution of  $x$  is, consequently, at most  $S(x)$ ). The idea of inferring contributions from score gaps will become important later.

**Dropping monotonicity** Since monotonicity can be violated, we emphasize that the upper bound  $e^{-|S(y)-S(x)|_+}$  for the probability of generating a larger downstream anomaly also holds without monotonicity in the following sense:

**Lemma 4.4** *For any  $\tilde{s}_X \leq S(y) - 1$ , the conditional probability  $P(S(Y) \geq S(y) | S(X) = S(x))$  with  $S(x) \geq \tilde{s}_X$  is smaller than  $e^{S(x) - S(y)}$  on the average over the interval  $[\tilde{s}_X, S(y)]$ , when averaging with respect to the conditional probability density  $P(S(X) = S(x) | S(y) \geq S(X) \geq \tilde{s}_X)$ .*

Although we cannot guarantee that  $P(S(Y) \geq S(y) | S(X) = S(x)) \leq e^{-|S(y)-S(x)|_+}$  for any *particular*  $S(x)$ , we can conclude that the bound is likely to hold approximately for a randomly chosen  $S(x)$ :

**Lemma 4.5** *Let  $P(X)$  have a probability density with respect to the Lebesgue measure, and let  $S(x)$  be randomly chosen from some interval  $[\tilde{s}_X, S(y)]$  according to the conditional distribution  $P(S(X) = S(x) | S(X) \geq S(x))$ . Then we obtain with probability at least  $1 - 1/c$  a score  $S(x)$  for which the following inequality holds:*

$$P\{S(Y) \geq S(y) | S(X) = S(x)\} \leq c \cdot e^{S(x) - S(y)}$$

The proof is an immediate consequence of Markov's inequality and Lemma 4.4. Note that we need to average over an interval  $[\tilde{s}_X, S(y)]$  of at least length 1 because the inequality does not need to hold locally for every small interval.

**Small sample version** When the anomaly scores are estimated from a *small* number of observations according to Eq.5, comparison of scores can still be insightful: if  $\hat{S}(y) \gg \hat{S}(x)$ , then for a large fraction of observations  $(\tilde{x}, \tilde{y})$  for which  $\tau(\tilde{x}) \geq \tau(x)$  the statement  $\tau(\tilde{y}) \geq \tau(y)$  does not hold. Hence, the event  $\tau(\tilde{x}) \geq \tau(x)$  is not a *sufficient cause* [46] for the event  $\tau(\tilde{y}) \geq \tau(y)$ . In this sense, we can still exclude the value with a smaller score as a candidate for the root cause, if we are interested in *sufficient* causes.

## 4.2 Outliers in DAGs with Multiple Nodes

To infer which node in a DAG with  $n$  nodes has been corrupted, we start with the hypothesis that all nodes except  $j$  worked as expected:  $H_0^j$ : for the anomaly event  $(x_1, \dots, x_n)$  all  $x_i$  with  $i \neq j$  have been drawn from  $P(X_i | Pa_i = pa_i)$ . To define a test statistics, we first introduce the *conditional* outlier scores from the arxiv version of [23]:

$$S(x_i | pa_i) := -\log P(\tau(X_i) \geq \tau(x_i) | Pa_i = pa_i),$$

where  $\tau$  is some feature function as before (we actually allow variable-dependent feature functions  $\tau_i$ , but they need to coincide between conditional and unconditional outlier scores). With variable input  $x_i, pa_i$ , they define random variables  $S(X_i | Pa_i)$ . Further, we add the following assumption to Monotonicity and Injectivity from Subsection 4.1:

3. **Continuity:** all variables  $X_i$  are continuous with density w.r.t. the Lebesgue measure, and also all conditional distributions  $P(X_i|Pa_i = pa_i)$  have such a density.

This condition ensures that all the conditional outlier scores are distributed according to the density  $p(s) = e^{-s}$ , because then the cumulative distribution function is uniformly distributed. It entails a property that will be convenient for testing  $H_0^j$ :

**Lemma 4.6** *Subject to the continuity assumption,  $\{S(X_1|Pa_1), \dots, S(X_n|Pa_n)\}$  are independent random variables.*

Independence of conditional scores enables the definition of a simple test statistics that is obtained by summing over the individual ones<sup>9</sup> together with a correction term. With the *cumulative (conditional) score*:  $S_{cum} := \sum_{i \neq j} S(X_i|Pa_i)$ , we have that:

$$S := S_{cum} - \log \sum_{l=0}^{n-2} \frac{S_{cum}^l}{l!}. \quad (10)$$

See Theorem [1] in the arxiv version of [23] for the proof. To understand Eq.10, note that the second term is needed to ‘recalibrate’ since the sum of independent IT scores is no longer an IT score, but with the extra term, it is. Intuitively, one may think of the extra term as a multi-hypothesis testing correction: the sum of independent IT scores is likely to be large because it is not unlikely that the set contains one large term. The following result states that this is quantitatively the right correction:

**Lemma 4.7** *If  $H_0^j$  holds, Eq. 10 is distributed according to the density  $p(s) = e^{-s}$ .*

As a direct result of the above lemmas we have:

**Theorem 4.8**  $H_0^j$  can be rejected for the observation  $(x_1, \dots, x_n)$  with *p-value*  $p = e^{-S_{cum}} \cdot \sum_{l=1}^{n-2} \frac{S_{cum}^l}{l!}$ .

The theorem justifies choosing the index  $j$  with the maximal conditional outlier score as the root cause, whenever we follow the working hypothesis that only one mechanism is corrupted.

We started this subsection with the goal of avoiding the estimation of conditional probabilities. Therefore, we will now replace conditional outlier scores with bounds derived from *marginal* anomaly scores, following the ideas from the bivariate case. To this end, we replace the monotonicity assumption from there with two stronger ones. We introduce the ‘outlier events’  $E_i := \{\tau(X_i) \geq \tau(x_i)\}$  and postulate:

1a. **Monotonicity:**

$$P\{E_n | \tau(Pa_i) = \tau(pa_i)\} \leq P\{E_n | \tau(Pa_i^1) \geq \tau(pa_i^1), \dots, \tau(Pa_i^k) \geq \tau(pa_i^k)\},$$

1b. **Non-negative dependence:** For any  $k$  nodes  $\{i_1, \dots, i_k\}$ :  $P(E_{i_1}, \dots, E_{i_k}) \geq P(E_{i_1}) \cdots P(E_{i_k})$ ,

where  $Pa_i^1, \dots, Pa_i^k$  denote the parents of  $X_i$ . Both conditions are close in spirit because they assume mutual positive influence of outlier events. While 1a is explicitly causal, 1b is actually a purely statistical condition, but also justified by an implicit causal model in which outliers at one point of the system render outliers at other points more likely and not less. We then obtain the following bound on the joint statistics:

**Theorem 4.9** *With the cumulative anomaly score increments:  $\hat{S}_{cum} = -\sum_{i \neq j} |S(x_i) - \sum_l S(pa_i^l)|_+$ , it holds that if conditions 1a and 1b hold,  $H_0^j$  can be rejected with  $p \leq e^{-\hat{S}_{cum}} \cdot \sum_{l=1}^{n-2} \frac{\hat{S}_{cum}^l}{l!}$ .*

Theorem 4.9 has interesting consequences for the scenario where  $n$  variables form the causal chain

$$X_1 \rightarrow X_2 \cdots \rightarrow X_n. \quad (11)$$

<sup>9</sup>Note that this resembles known methods of aggregating p-values, but on a logarithmic scale [47].

In this case,  $\hat{S}_{\text{cum}}$  reduces to the sum of score differences for adjacent nodes. Accordingly,  $H_0^j$  can then be rejected at p-value:

$$p \leq \begin{cases} e^{-S(x_1) - \sum_{i \neq j, i \geq 2} |S(x_i) - S(x_{i-1})|_+} & \text{for } i \neq 1 \\ e^{-\sum_{i \geq 2} |S(x_i) - S(x_{i-1})|_+} & \text{for } i = 1 \end{cases} \quad (12)$$

We conclude that  $H_0^j$  needs to be rejected whenever the anomaly score increases significantly along the chain of anomalies at any  $i \neq j$ . This justifies inferring the index  $j$  as the unique root cause that maximizes the score difference  $|S(x_j) - S(x_{j-1})|_+$  (with the difference being  $|S(x_1) - 0|_+ = S(x_1)$  for the first node with ‘an imaginary non-anomalous node’  $X_0$ ) because this yields the weakest bound as in Eq.12. Motivated by these bounds, we propose the algorithm SMOOTH TRAVERSAL which selects the node as the root cause that shows the strongest increase in anomaly score compared to its most anomalous parent. In contrast to the usual Traversal [27, 28, 9], this avoids choosing an arbitrary threshold above which a node is considered anomalous. We can prove that SMOOTH TRAVERSAL identifies the correct root cause in a causal chain under a condition that is a slight extension of Definition 3.3:

**Theorem 4.10** *Let  $X_1, \dots, X_n$  be connected by the causal chain (4.2) and node  $j \in \{1, \dots, n\}$  be the unique root cause of the anomaly  $x_n$  as in Definition 3.3 and all nodes before  $j$  have small anomaly score, i.e.,  $S(x_i) \leq S(x_n)/4$ . Then we have:*

$$\begin{aligned} S(x_j) - S(x_{j-1}) &\geq S(x_n)/2 \\ S(x_i) - S(x_{i-1}) &\leq S(x_n)/4 \quad \forall i \neq j, i \geq 2. \end{aligned}$$

Hence, the root cause  $j$  is the unique node that maximizes the anomaly gap to its parent.

The additional condition that all ancestors of the root cause have low scores does not follow from the earlier assumption stating that they have low contribution. However, since we assume that all mechanisms except  $j$  work as usual, we indeed expect no anomalies further upstream (unless  $j$  is so large that some high scores become likely).

Note the analogy to TOCA, where we maximized the gap of logarithmic conditional probabilities, while we maximize the gap of outlier scores here, which simplifies the analysis drastically. Restricting the attention to a causal chain may not reduce generality as much as it seems at first glance. After all, our root cause analysis would backtrack anomalies from the target node upstream in the direction of the largest anomalies and ignore branches of side-effects that do not cross the target node. Note that monotonicity condition could also be avoided here. Then we would again obtain bounds that hold for most observations up to some  $\epsilon$  resulting in slightly less concise inequalities.

### 4.3 Shortlist of Root Causes via Ordering Anomaly Scores

We now drop the final assumption and assume that the causal DAG is not known and we are only given the marginal anomaly scores  $S(x_1), \dots, S(x_n)$  of each node. How can we find the root cause? We now argue that the top-scored anomalies provide a short list of root causes. The idea is, again, that the anomaly  $x_i$  is unlikely to cause the downstream anomaly  $x_k$  if  $S(x_i) \ll S(x_k)$ , unless we allow additional mechanisms (except for  $i$ ) to be corrupted. To show this, we restrict the attention to a DAG with three nodes, in which we have merged all paths from  $X_i$  to  $X_k$  to the arrow  $X_i \rightarrow X_k$  and all nodes upstream of  $X_i$  to a single huge confounder  $X_l$ . In analogy to the proof of Theorem 4.9 and with the same assumptions, we can bound conditional outlier score with the score difference to the sum the parent scores:  $S(x_k|x_i, x_l) \geq |S(x_k) - S(x_i) - S(x_l)|_+$ . Assuming  $S(x_l) \approx 0$ , the hypothesis that the mechanism  $P(X_k|X_i, X_l)$  worked as expected, can be rejected at a p-level of about  $e^{-|S(x_k) - S(x_i)|_+}$ . This motivates the algorithm SCORE ORDERING which chooses top-scored anomalies as candidates for root causes. We do not provide pseudocode due to its simplicity.

## 5 Experiments

We provide a comparison of the performance of our proposed algorithms together with other baselines on simulated and real-world data. We provide a short description of each of the algorithms below:

- TOCA (ours, refer to Algorithm 1) it traverses in the topological ordering of the nodes and identifies the node with the highest jump in estimated log probabilities as the root cause.
- SMOOTH TRAVERSAL (ours, refer to Section 4.2) identifies the node that shows strongest increase of anomaly score compared to its most anomalous parent as the root cause.
- SCORE ORDERING (ours, refer to Section 4.3) takes only the node with the highest anomaly score as the root cause. It is the only approach that does not require the causal graph or SCM and uses only the estimated anomaly scores.
- ‘Traversal’ [9, 27, 28] identifies a node as a root cause under the two conditions: 1) none of its parents exhibit anomalous behaviour, and 2) it is linked to the anomalous target node through a path of anomalous nodes.
- Circa [25] fits a linear Gaussian SCM to the data in the non-anomalous regime and compares the predicted value of each variable, given its parents (hence, it uses the causal graph), to the observed value in the anomalous regime. The node whose value differs the most is identified as the root cause.
- Counterfactual [23] finds the Shapley contribution of each node to the outlieriness in the target through full counterfactual analysis and outputs the node with the highest Shapley value.

We assume that only a single data point is available in the anomalous regime. We, therefore, do not compare with approaches that involve learning the causal graph (e.g., Root Cause Discovery [31]), nor do we compare with approaches such as  $\varepsilon$ -Diagnosis [11] which perform two-sample tests to identify which nodes have changed significantly from the non-anomalous to the anomalous regimes. We generate random SCM with 50 nodes with linear and non-linear structural equations (more details on the generation process in Appendix C) and sample 1000 observations of the SCM for the non-anomalous regime to train the IT anomaly scorer (as in Eq. 5). To produce anomalous data we choose a root cause at random from the list of all nodes and a target node from the set of its descendants (including itself). Second, we sample the noise of all variables and modify the noise of the root cause by adding  $x$  standard deviations, where  $x \in \{2, 2.1, \dots, 3\}$ , and propagate the noises through the SCM to obtain a realization of each variable. We repeat this process 100 times for each  $x$  value and consider the algorithm successful if its top-ranking result coincides with the chosen root cause. Through our experiments on synthetic data, we aim to answer the following questions:

**How does performance of each algorithm depend on the strength of the anomaly at the root cause?** Refer to Fig. 1 for a comparison of the performance of different algorithms against the strength of the anomaly at the root cause. We find that the strongest performing algorithms are SMOOTH TRAVERSAL, Traversal, and Counterfactual, all of which outperform SCORE ORDERING. Circa performs considerably worse than the other approaches which we suspect is due to the assumption of linearity. The performance of SCORE ORDERING improves as the anomaly strength increases. This is expected as the algorithm aims to find the *unique* anomalous node.

**How do the runtimes of each method scale with increasing graph size?** For a fixed strength of the injected perturbation to the root cause (3 standard deviations away from its mean), we measure the runtime of each algorithm for SCMs with an increasing number of nodes, generated similarly as described above. We observe that (refer to Fig. 2 in Appendix C), Traversal and SMOOTH TRAVERSAL are the fastest, with the remaining approaches having comparable average runtimes.

**How is performance affected by increasing graph size?** We generate SCMs with the number of nodes in the set  $\{20, 40, \dots, 100\}$  with a fixed amount of injected perturbation to the root cause (3 standard deviations away from its mean). In Fig. 3 in Appendix C we see that the performance of SCORE ORDERING slightly decreases with the size of the SCM.

Refer to Appendix C.3 for a comparison of the algorithms in terms of their practicality. We evaluated the algorithms on a real-world dataset, the ‘PetShop dataset’ [29]. We include the results in the Appendix C.4.

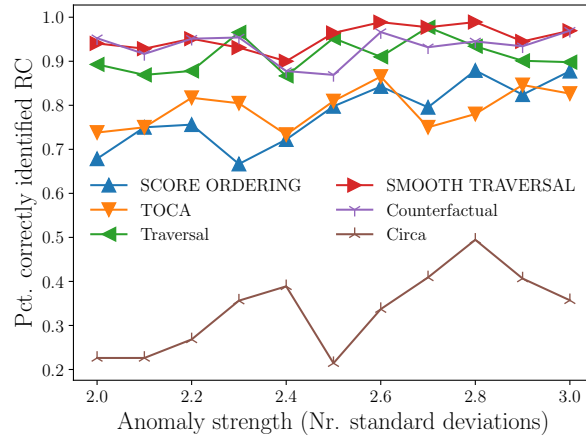


Figure 1: True positive rate of the compared algorithms in identifying the root cause with known structural assignments against the strength of the perturbation injected at the root cause node.

## 6 Conclusions

We have explored several directions in which the practical limitations of RCA can be mitigated without sacrificing too much of its theoretical justification provided in earlier works. First, by avoiding rung 3 causal models and high computational load, second by avoiding estimation of conditional probabilities, and third by not even relying on the causal DAG.

## Acknowledgements

We would like to thank Manuel Gomez-Rodriguez for fruitful discussions during different stages of the project.

## References

- [1] S Wibisono, MT Anwar, Aji Supriyanto, and IHA Amin. Multivariate weather anomaly detection using dbscan clustering algorithm. In *Journal of Physics: Conference Series*, volume 1869, page 012077. IOP Publishing, 2021.
- [2] Eric V Strobl and Thomas A Lasko. Identifying patient-specific root causes with the heteroscedastic noise model. *Journal of Computational Science*, 72:102099, 2023.
- [3] Eric V Strobl. Counterfactual formulation of patient-specific root causes of disease. *Journal of Biomedical Informatics*, page 104585, 2024.
- [4] Gian Antonio Susto, Matteo Terzi, and Alessandro Beghi. Anomaly detection approaches for semiconductor manufacturing. *Procedia Manufacturing*, 11:2018–2024, 2017.
- [5] Jellis Vanhoeyveld, David Martens, and Bruno Peeters. Value-added tax fraud detection with scalable anomaly detection techniques. *Applied Soft Computing*, 86:105895, 2020.
- [6] Sanjiv Das, Richard Stanton, and Nancy Wallace. Algorithmic fairness. *Annual Review of Financial Economics*, 15:565–593, 2023.

- [7] Dongjie Wang, Zhengzhang Chen, Jingchao Ni, Liang Tong, Zheng Wang, Yanjie Fu, and Haifeng Chen. Hierarchical graph neural networks for causal discovery and root cause localization. *arXiv preprint arXiv:2302.01987*, 2023.
- [8] Cheng-Ming Lin, Ching Chang, Wei-Yao Wang, Kuang-Da Wang, and Wen-Chih Peng. Root cause analysis in microservice using neural granger causal discovery. *arXiv preprint arXiv:2402.01140*, 2024.
- [9] Dewei Liu, Chuan He, Xin Peng, Fan Lin, Chenxi Zhang, Shengfang Gong, Ziang Li, Jiayu Ou, and Zheshun Wu. Microhecl: high-efficient root cause localization in large-scale microservice systems. In *Proceedings of the 43rd International Conference on Software Engineering: Software Engineering in Practice, ICSE-SEIP '21*, page 338–347. IEEE Press, 2021.
- [10] Azam Ikram, Sarthak Chakraborty, Subrata Mitra, Shiv Saini, Saurabh Bagchi, and Murat Kocaoglu. Root cause analysis of failures in microservices through causal discovery. *Advances in Neural Information Processing Systems*, 35:31158–31170, 2022.
- [11] Huasong Shan, Yuan Chen, Haifeng Liu, Yunpeng Zhang, Xiao Xiao, Xiaofeng He, Min Li, and Wei Ding.  $\epsilon$ -diagnosis: Unsupervised and real-time diagnosis of small-window long-tail latency in large-scale microservice platforms. In *The World Wide Web Conference*, pages 3215–3222, 2019.
- [12] Meng Ma, Jingmin Xu, Yuan Wang, Pengfei Chen, Zonghua Zhang, and Ping Wang. Automap: Diagnose your microservice-based web applications automatically. In *Proceedings of The Web Conference 2020*, pages 246–258, 2020.
- [13] Douglas M Hawkins. *Identification of outliers*, volume 11. Springer, 1980.
- [14] Varun Chandola, Arindam Banerjee, and Vipin Kumar. Anomaly detection: A survey. *ACM computing surveys (CSUR)*, 41(3):1–58, 2009.
- [15] Charu C Aggarwal. *An introduction to outlier analysis*. Springer, 2017.
- [16] Ane Blázquez-García, Angel Conde, Usue Mori, and Jose A Lozano. A review on outlier/anomaly detection in time series data. *ACM Computing Surveys (CSUR)*, 54(3):1–33, 2021.
- [17] Leman Akoglu. Anomaly mining: Past, present and future. In *Proceedings of the 30th ACM International Conference on Information & Knowledge Management*, pages 1–2, 2021.
- [18] Edwin M Knorr and Raymond T Ng. Finding intensional knowledge of distance-based outliers. In *Vldb*, volume 99, pages 211–222, 1999.
- [19] Barbora Micenková, Raymond T Ng, Xuan-Hong Dang, and Ira Assent. Explaining outliers by subspace separability. In *2013 IEEE 13th international conference on data mining*, pages 518–527. IEEE, 2013.
- [20] Ninghao Liu, Donghwa Shin, and Xia Hu. Contextual outlier interpretation. *arXiv preprint arXiv:1711.10589*, 2017.
- [21] Meghanath Macha and Leman Akoglu. Explaining anomalies in groups with characterizing subspace rules. *Data Mining and Knowledge Discovery*, 32:1444–1480, 2018.
- [22] Nikhil Gupta, Dhivya Eswaran, Neil Shah, Leman Akoglu, and Christos Faloutsos. Beyond outlier detection: Lookout for pictorial explanation. In *Machine Learning and Knowledge Discovery in Databases: European Conference, ECML PKDD 2018, Dublin, Ireland, September 10–14, 2018, Proceedings, Part I 18*, pages 122–138. Springer, 2019.
- [23] Kailash Budhathoki, Lenon Minorics, Patrick Bloebaum, and Dominik Janzing. Causal structure-based root cause analysis of outliers. In Kamalika Chaudhuri, Stefanie Jegelka, Le Song, Csaba Szepesvari, Gang Niu, and Sivan Sabato, editors, *Proceedings of the 39th International Conference on Machine Learning*, volume 162 of *Proceedings of Machine Learning Research*, pages 2357–2369. PMLR, 17–23 Jul 2022.

- [24] Dongjie Wang, Zhengzhang Chen, Jingchao Ni, Liang Tong, Zheng Wang, Yanjie Fu, and Haifeng Chen. Interdependent causal networks for root cause localization. In *Proceedings of the 29th ACM SIGKDD Conference on Knowledge Discovery and Data Mining*, pages 5051–5060, 2023.
- [25] Mingjie Li, Zeyan Li, Kanglin Yin, Xiaohui Nie, Wenchi Zhang, Kaixin Sui, and Dan Pei. Causal inference-based root cause analysis for online service systems with intervention recognition. In *Proceedings of the 28th ACM SIGKDD Conference on Knowledge Discovery and Data Mining*, pages 3230–3240, 2022.
- [26] Dongjie Wang, Zhengzhang Chen, Yanjie Fu, Yanchi Liu, and Haifeng Chen. Incremental causal graph learning for online root cause analysis. In *Proceedings of the 29th ACM SIGKDD Conference on Knowledge Discovery and Data Mining*, pages 2269–2278, 2023.
- [27] Pengfei Chen, Yong Qi, Pengfei Zheng, and Di Hou. Causeinfer: Automatic and distributed performance diagnosis with hierarchical causality graph in large distributed systems. In *IEEE INFOCOM 2014 - IEEE Conference on Computer Communications*, pages 1887–1895, 2014.
- [28] JinJin Lin, Pengfei Chen, and Zibin Zheng. Microscope: Pinpoint performance issues with causal graphs in micro-service environments. In *International Conference on Service Oriented Computing*, 2018.
- [29] Michaela Hardt, William Orchard, Patrick Blöbaum, Shiva Kasiviswanathan, and Elke Kirschbaum. The petshop dataset – finding causes of performance issues across microservices, 2023.
- [30] Yu Gan, Mingyu Liang, Sundar Dev, David Lo, and Christina Delimitrou. Sage: practical and scalable ml-driven performance debugging in microservices. In *Proceedings of the 26th ACM International Conference on Architectural Support for Programming Languages and Operating Systems, ASPLOS '21*, page 135–151, New York, NY, USA, 2021. Association for Computing Machinery.
- [31] Azam Ikram. Sock-shop data. <https://github.com/azamikram/rcd/tree/master/sock-shop-data>, 2023.
- [32] Jin Tian and Judea Pearl. Causal discovery from changes. In *UAI*, 2001.
- [33] Kun Zhang, Biwei Huang, Jiji Zhang, Clark Glymour, and Bernhard Schölkopf. Causal discovery from nonstationary/heterogeneous data: Skeleton estimation and orientation determination. In *Proceedings of the Twenty-Sixth International Joint Conference on Artificial Intelligence, IJCAI-17*, pages 1347–1353, 2017.
- [34] Amin Jaber, Murat Kocaoglu, Karthikeyan Shanmugam, and Elias Bareinboim. Causal discovery from soft interventions with unknown targets: Characterization and learning. In H. Larochelle, M. Ranzato, R. Hadsell, M.F. Balcan, and H. Lin, editors, *Advances in Neural Information Processing Systems*, volume 33, pages 9551–9561. Curran Associates, Inc., 2020.
- [35] Nicola Gnecco, Nicolai Meinshausen, Jonas Peters, and Sebastian Engelke. Causal discovery in heavy-tailed models. *The Annals of Statistics*, 49(3):1755 – 1778, 2021.
- [36] Carlos Améndola, Benjamin Hollering, Seth Sullivant, and Ngoc Tran. Markov equivalence of max-linear Bayesian networks. In Cassio de Campos and Marloes H. Maathuis, editors, *Proceedings of the Thirty-Seventh Conference on Uncertainty in Artificial Intelligence*, volume 161 of *Proceedings of Machine Learning Research*, pages 1746–1755. PMLR, 27–30 Jul 2021.
- [37] J. Pearl and J. Mackenzie. *The book of why*. Basic Books, USA, 2018.
- [38] J. Pearl. *Causality*. Cambridge University Press, 2000.
- [39] Julius Von Kügelgen, Abdirisak Mohamed, and Sander Beckers. Backtracking counterfactuals. In Mihaela van der Schaar, Cheng Zhang, and Dominik Janzing, editors, *Proceedings of the Second Conference on Causal Learning and Reasoning*, volume 213 of *Proceedings of Machine Learning Research*, pages 177–196. PMLR, 11–14 Apr 2023.

- [40] Kun Zhang, Zhikun Wang, Jiji Zhang, and Bernhard Schölkopf. On estimation of functional causal models: general results and application to the post-nonlinear causal model. *ACM Transactions on Intelligent Systems and Technology (TIST)*, 7(2):1–22, 2015.
- [41] A. Balke and J. Pearl. Counterfactual probabilities: Computational methods, bounds, and applications. In R. Lopez D. Mantaras and D. Poole, editors, *Uncertainty in Artificial Intelligence*, volume 10. Morgan Kaufmann, San Mateo, 1994.
- [42] Akash Maharaj, Ritwik Sinha, David Arbour, Ian Waudby-Smith, Simon Z. Liu, Moumita Sinha, Raghavendra Addanki, Aaditya Ramdas, Manas Garg, and Viswanathan Swaminathan. Anytime-valid confidence sequences in an enterprise a/b testing platform. In *Companion Proceedings of the ACM Web Conference 2023*, WWW '23 Companion, page 396–400, New York, NY, USA, 2023. Association for Computing Machinery.
- [43] Dominik Janzing, Patrick Blöbaum, Atalanti A Mastakouri, Philipp M Faller, Lenon Minorics, and Kailash Budhathoki. Quantifying intrinsic causal contributions via structure preserving interventions. In *International Conference on Artificial Intelligence and Statistics*, pages 2188–2196. PMLR, 2024.
- [44] Yoshua Bengio, Tristan Deleu, Nasim Rahaman, Rosemary Ke, Sébastien Lachapelle, Olexa Bilaniuk, Anirudh Goyal, and Christopher Pal. A meta-transfer objective for learning to disentangle causal mechanisms. *arXiv preprint arXiv:1901.10912*, 2019.
- [45] B. Schölkopf, F. Locatello, S. Bauer, N. R. Ke, N. Kalchbrenner, A. Goyal, and Y. Bengio. Toward causal representation learning. *Proceedings of the IEEE*, 109(5):612–634, 2021.
- [46] Judea Pearl. Sufficient causes: On oxygen, matches, and fires. *Journal of Causal Inference*, 7(2), 2019.
- [47] R. A. Fisher. *Statistical Methods for Research Workers*. Oliver and Boyd, 1925.
- [48] J. D. Hunter. Matplotlib: A 2d graphics environment. *Computing in Science & Engineering*, 9(3):90–95, 2007.

---

**Algorithm 1 (TOCA)** Returns the unique root cause of the outlier  $x_n$ , as define by Def. 3.3.

---

```

1: Input: outlier  $x_n$ , the FCM between the variables  $X_1, \dots, X_n$ , a topological ordering of nodes  $\pi$ 
2: Initialize:  $\mathcal{A} = \{0\}_{i=1}^n$ 
3: for  $\text{itr} \in \{1, \dots, k\}$  do
4:    $\tilde{\mathbf{n}} = (n'_1, \dots, n'_n)$  {Sampled from the normal mechanism}
5:    $\mathcal{S} = \emptyset$ 
6:   for  $i \in \pi$  do
7:      $\mathcal{S} \rightarrow \mathcal{S} \cup \{i\}$ 
8:      $\mathcal{A}_i \leftarrow \mathcal{A}_i + \mathbb{I}[\tau(F(\tilde{\mathbf{n}}_{\mathcal{U} \setminus \mathcal{S}}, \mathbf{n}_{\mathcal{S}})) \geq \tau(x_n)]$ 
9:   end for
10: end for
11: return  $\operatorname{argmax}_{i \in \{1, \dots, n\}} \log \frac{\mathcal{A}_{i-1}}{\mathcal{A}_i}$ 

```

---

## A ANALYSIS OF TOPOLOGICALLY ORDERED CONTRIBUTION ANALYSIS (TOCA) 1

Refer to Algorithm box 1 for a pseudocode of TOCA.

### A.1 Properties of TOCA

**Conceptual difference to traversal algorithm:** First remember that traversal-based approach [27, 28, 9] identifies a node as a root cause under two conditions: 1) none of its parent nodes exhibits anomalous behavior and 2) it is linked to the anomalous target node through a path of anomalous nodes. When we identify a node  $j$  for which the log probabilities of  $E$  jump when including  $j$  in the conditioning set, we can be certain that  $j$  is a root cause in the sense of having high contribution. This is not the case for the traversal algorithm (as used by [27, 28, 9]), which infers the most upstream anomaly as root cause. Let, for instance let  $X_1 = N_1$  and  $X_2 = 0.1 \cdot X_1 + N_2$ , where  $X$  and  $N_2$  are standard Gaussians  $\mathcal{N}(0, 1)$ . When  $x_1 = -3$  and  $x_2 = 3$ , traversal identifies  $x_1$  as the root cause (because both values  $x_1$  and  $x_2$  are anomalous), although a more typical value of  $X_1$  would have made the target outlier  $x_2$  *even stronger*. Hence,  $x_1$  has even a negative contribution in the above sense.

**Why do we measure gaps of log probabilities?** From the perspective of statistical estimation, it would certainly be easier to seek for the index with the largest increase of probability instead of the largest increase of *logarithmic* probability of  $E$ . Why don't we work with a definition of contribution that is defined by *additive* increase rather than *multiplicative* increase? The following example shows that high multiplicative increase can only be caused by *rare* events, while high additive increase can happen quite frequently: Consider the boolean causal relation between 3 binaries  $E = N_1 \wedge N_2$  with  $P(N_1 = 1) = 1/2$  while  $P(N_2 = 1) = 0.001$ . Then we have  $P(E = 1 | N_2 = 1) = 1/2$ , while  $P(E = 1 | N_1 = 1, N_2 = 1) = 1$ . Hence,  $n_1 = 1$  increases the probability of  $E$  by  $1/2$ , although this value occurs quite frequently. In contrast, a large *multiplicative* increase is only achieved by the *rare* event  $n_2 = 1$  (in agreement with Proposition 3.2). The conclusion that large contribution comes from a corrupted mechanism ('the root cause') is only justified because high contributions are unlikely otherwise.

### A.2 Sample Complexity of TOCA

To reliably tell whether  $P(E | n_1, \dots, n_i)$  is smaller or equal to  $e^{-\frac{3}{4}S(x_n)}$  or greater or equal to  $e^{-\frac{1}{4}S(x_n)}$  we need to estimate it up to an error of

$$\frac{1}{2}(e^{-\frac{1}{4}S(x_n)} - e^{-\frac{3}{4}S(x_n)}) = \frac{1}{2}(e^{-\frac{1}{4}S(x_n)} - (e^{-\frac{1}{2}S(x_n)}e^{-\frac{1}{4}S(x_n)})) \stackrel{i}{\geq} \frac{1}{4}e^{-\frac{1}{4}S(x_n)} := \delta, \quad (13)$$

where (i) is due to the assumption that  $e^{-S(x_n)/2} \leq 1/2$ , since otherwise  $S(x_n)$  is too small to be considered an outlier. We investigate how many samples we need to estimate the probabilities  $P(E | n_1, \dots, n_i)$  up to error level  $\delta$ :

**Lemma A.1** *If we use at least  $k = \log \frac{2n}{\alpha} / (2\delta^2)$  number of data samples, the empirical probabilities  $\hat{P}$  satisfy  $|\hat{P}(E | n_1, \dots, n_i) - P(E | n_1, \dots, n_i)| < \delta \forall i \leq n$  with probability at least  $1 - \alpha$ .*

**Proof** The proof simply follows by using Hoeffding's bound together with union bound, if  $k$  data points are used for estimation of each  $P(E | \mathbf{n}_{I^{\pi < i}})$ , we have based on Hoeffding's bound for each  $i$  that:

$$P\left(|\hat{P}(E | \mathbf{n}_{I^{\pi < i}}) - P(E | \mathbf{n}_{I^{\pi < i}})| < \delta\right) > 1 - 2e^{-2k\delta^2},$$

From union bound we have that it simultaneously holds for all  $i$  with probability at least  $1 - 2ne^{-2k\delta^2}$ . To have  $1 - 2ne^{-2k\delta^2} > 1 - \alpha$  we should have:

$$2ne^{-2k\delta^2} < \alpha \quad \Rightarrow \quad k > \frac{\log \frac{2n}{\alpha}}{2\delta^2}$$

■

As an example, for  $\alpha = 0.1$  and using  $n = 50$  nodes, we would need  $\approx 80e^{S(x_n)/2}$  number of data sample. Since we estimate  $n$  different probabilities,  $\alpha$  needs to be chosen such that  $n\alpha$  is smaller than the desired probability of failure. Note that the arguments above implicitly assume that we have learned a structural equation model (SCM) that reproduces the correct conditional probabilities when the noise variables are correctly randomized. It is hard to provide error guarantees for the SCM. Given this assumption, we could sample as many instances of the noise variables as we like if we knew the distributions  $P(N_j)$ . In absence of this knowledge, we choose all available values (reconstructed via inverting the SCM) for each  $N_j$ . This way, estimation accuracy for  $P(E | n_1, \dots, n_i)$  is limited by the observed sample size.

## B PROOFS

### B.1 Proof of Proposition 2.1

With the event  $E$  as in Eq. 3 and  $C^\pi(j) := C(j | I^{\pi < j})$  we have

$$\begin{aligned} C^\pi(j) &= \log \frac{P(E | \mathbf{N}_{\pi < j \cup \{j\}} = \mathbf{n}_{\pi < j \cup \{j\}})}{P(E | \mathbf{N}_{\pi < j} = \mathbf{n}_{\pi < j})} \stackrel{i}{=} \log \frac{P(E | \mathbf{X}_{\pi < j \cup \{j\}} = \mathbf{x}_{\pi < j \cup \{j\}})}{P(E | \mathbf{X}_{\pi < j} = \mathbf{x}_{\pi < j})} \\ &\stackrel{ii}{=} \log \frac{P(E | do(\mathbf{X}_{\pi < j \cup \{j\}} = \mathbf{x}_{\pi < j \cup \{j\}}))}{P(E | do(\mathbf{X}_{\pi < j} = \mathbf{x}_{\pi < j}))}. \end{aligned} \quad (14)$$

(i) and (ii) are seen as follows:

$$P(E | \mathbf{N}_{\mathcal{I}}) = P(E | \mathbf{X}_{\mathcal{I}}) = P(E | do(\mathbf{X}_{\mathcal{I}})). \quad (15)$$

The first equality in Eq. 15 follows from  $X_n \perp X_{\mathcal{I}} | \mathbf{N}_{\mathcal{I}}$  and because  $\mathbf{X}_{\mathcal{I}}$  is a function of  $\mathbf{N}_{\mathcal{I}}$ . The second one follows because conditioning on all ancestors blocks all backdoor paths. Note that since  $\pi$  is a topological ordering of the nodes all  $\pi < j$  are ancestors of  $j$ .

## B.2 Proof of Lemma 3.1

Denote  $q(\mathcal{S}) = P(E | \mathbf{N}_S = \mathbf{n}_S)$  then we have that

$$\begin{aligned} C(\mathcal{R}|\mathcal{S}) &= \log q(\mathcal{S} \cup \mathcal{R}) - \log q(\mathcal{S}) \\ &= (\log q(\mathcal{S} \cup \mathcal{R}) - \log q(\mathcal{S} \cup \mathcal{R} \setminus \{j_k\})) + (\log q(\mathcal{S} \cup \mathcal{R} \setminus \{j_k\}) - \log q(\mathcal{S} \cup \mathcal{R} \setminus \{j_k, j_{k-1}\})) + \dots \\ &\quad + (\log q(\mathcal{S} \cup \{j_1\}) - \log q(\mathcal{S})) = C(j_1|\mathcal{S}) + \sum_{i=2}^k C(j_i|\mathcal{S} \cup \{j_1, \dots, j_{i-1}\}). \end{aligned}$$

## B.3 Proof of Proposition 3.2

By definition we have that

$$C(\mathcal{R}|\mathcal{S}) = \log \frac{P(E|\mathbf{N}_R = \mathbf{n}_R, \mathbf{N}_S = \mathbf{n}_S)}{P(E|\mathbf{N}_S = \mathbf{n}_S)},$$

and we use  $P(E|\mathbf{n}_S)$  instead of  $P(E|\mathbf{N}_S = \mathbf{n}_S)$  when it is clear from the context.

Further,  $C(\mathcal{R}|\mathcal{S})$  is actually a function of  $\mathbf{n}_R$  and  $\mathbf{n}_S$ . For fixed  $\mathbf{n}_S$ , define the set  $B := \{\mathbf{n}_R | C(\mathcal{R}|\mathcal{S}) \geq \alpha\}$ . It can equivalently be described by

$$B = \{\mathbf{n}_R | \log \frac{P(E|\mathbf{n}_R, \mathbf{n}_S)}{P(E|\mathbf{n}_S)} \geq \alpha\} = \{\mathbf{n}_R | P(E|\mathbf{n}_R, \mathbf{n}_S) \geq P(E|\mathbf{n}_S) \cdot e^\alpha\}.$$

We thus have

$$P(E|\mathbf{n}_R \in B, \mathbf{n}_S) \geq P(E|\mathbf{n}_S) \cdot e^\alpha.$$

Hence,

$$\frac{P(E, \mathbf{n}_R \in B|\mathbf{n}_S)}{P(\mathbf{n}_R \in B|\mathbf{n}_S)} \geq P(E|\mathbf{n}_S) \cdot e^\alpha.$$

Using

$$P(E|\mathbf{n}_S) \geq P(E, \mathbf{n}_R \in B|\mathbf{n}_S)$$

we obtain

$$P(\mathbf{n}_R \in B|\mathbf{n}_S) \leq e^{-\alpha}.$$

## B.4 Proof of Theorem 3.4

For all  $i \in I^{\pi < j}$  we have that:

$$\begin{aligned} C(\{1, \dots, i-1\}|\emptyset) &= \log \frac{P(E|n_1, \dots, n_{i-1})}{P(E)} \\ &\Rightarrow P(E|n_1, \dots, n_{i-1}) = P(E)e^{C(\{1, \dots, i-1\}|\emptyset)} \stackrel{(a)}{\leq} e^{-\frac{3}{4}S(x_n)} \end{aligned}$$

where (a) follows from the fact that  $P(E) = e^{-S(X_n)}$  together with condition (i). For all  $i \in I^{\pi > j}$  we have that:

$$\begin{aligned} C(\{i+1, \dots, n\}|\{1, \dots, i\}) &= \log \frac{P(E|n_1, \dots, n_n)}{P(E|n_1, \dots, n_i)} = \log \frac{1}{P(E|n_1, \dots, n_i)} \\ &\Rightarrow P(E|n_1, \dots, n_i) = e^{-C(\{i+1, \dots, n\}|\{1, \dots, i\})} \stackrel{(a)}{\geq} e^{-\frac{1}{4}S(x_n)} \end{aligned}$$

where (a) is due to condition (ii). Therefore, log probabilities jump by at least  $S(x_n)/2$  for  $i = j$ . Furthermore, such a jump can never happen for any  $i \neq j$ .

## B.5 Proof of Lemma 4.4

Since we assume that  $S(X)$  is a continuous variable with density with respect to the Lebesgue measure, the density reads  $p(S(X) = s) = e^{-s}$  by construction of outlier scores. Accordingly, the conditional distribution of  $S(X)$ , given  $S(y) \geq S(X) \geq S(x)$  has the density  $p(S(X) = s | S(y) \geq S(X) \geq \tilde{s}_X) = e^{-s} / (e^{\tilde{s}_X} - e^{-S(y)})$ . We want to compare averages of the expressions

$$P(S(Y) \geq S(y) | S(X) = s) \quad \text{versus} \quad e^{-|S(y)-s|_+}$$

over the interval  $[\tilde{s}_X, S(y)]$ . Averaging the difference of the two expressions with respect to the above-mentioned density yields

$$\begin{aligned} & \int_{\tilde{s}_X}^{S(y)} \left( P(S(Y) \geq S(y) | S(X) = s) - e^{-|S(y)-s|_+} \right) p(S(x) | S(y) \geq S(X) \geq \tilde{s}_X) ds \\ &= P(S(Y) \geq S(y) | S(y) \geq S(X) \geq \tilde{s}_X) - \int_{\tilde{s}_X}^{S(y)} e^{s-S(y)} \frac{e^{-s}}{e^{-\tilde{s}_X} - e^{-S(y)}} ds \\ &\leq \frac{e^{-S(y)}}{e^{-\tilde{s}_X} - e^{-S(y)}} - \int_{\tilde{s}_X}^{S(y)} \frac{e^{-S(y)}}{e^{-\tilde{s}_X} - e^{-S(y)}} ds = \frac{e^{-S(y)}}{e^{-\tilde{s}_X} - e^{-S(y)}} (1 - S(y) + \tilde{s}_X) \leq 0. \end{aligned}$$

The first inequality holds because  $P(B|A) \leq P(B)/P(A)$  for any two events  $A, B$  and the second because we have assumed  $\tilde{s}_X \leq S(y) - 1$ .

## B.6 Proof of Lemma 4.6

Assume without loss of generality that  $X_1, \dots, X_n$  is a topological ordering of the DAG. Then  $S(X_i | X_1, \dots, X_{i-1}) = S(X_i | Pa_i)$  holds due to the local Markov condition. Since  $S(X_j | Pa_j = pa_j)$  has density  $e^{-s}$  for all  $pa_j$ , also  $S(X_i | X_1 = x_1, \dots, X_{i-1} = x_{i-1})$  has density  $e^{-s}$  for all  $x_1, \dots, x_{i-1}$ . Hence,  $S(X_i | Pa_i)$  is independent of  $X_1, \dots, X_{i-1}$ .

## B.7 Proof of Lemma 4.7

The proof follows from a minor modification of the proof of Lemma 1 in the arxiv version of [23] by replacing  $n$  with  $n - 1$ .

## B.8 Proof of Theorem 4.8

The theorem is a direct result of Lemma 4.6 and Lemma 4.7.

## B.9 Proof of Theorem 4.9

$$P(E_i | Pa_i = pa_i) \leq P(E_i | E_{Pa_i^1}, \dots, E_{Pa_i^k}) \leq \frac{P(E_i)}{P(E_{Pa_i^1}, \dots, E_{Pa_i^k})} \leq \frac{P(E_i)}{P(E_{Pa_i^1}) \cdots P(E_{Pa_i^k})}.$$

Recalling that anomaly scores are non-negative, we thus obtain:

$$S(x_i | pa_i) \geq |S(x_i) - \sum_{l=1}^k S(pa_i^l)|_+,$$

with the notation  $|a| := (a + |a|)/2$ . Hence, we obtain a lower bound for  $s_{cum}$ :

$$s_{cum} \geq \sum_{i \neq j} |S(x_i) - \sum_l S(pa_i^l)|_+ =: \hat{s}_{cum}. \quad (16)$$

## B.10 Proof of Theorem 4.10

By assumption, we have for all  $i \geq j$

$$\begin{aligned} \frac{1}{4} &\geq C(\{i+1, \dots, n\}|\{1, \dots, i\}) = \log \frac{P(S(X_n) \geq S(x_n)|x_1, \dots, x_n)}{P(S(X_n) \geq S(x_n)|x_1, \dots, x_i)} = -\log P(S(X_n) \geq S(x_n)|x_i) \\ &= -\log P(S(X_n) \geq S(x_n)|S(x_i) = S(x_i)) \geq |S(x_n) - S(x_i)|_+ - \epsilon. \end{aligned}$$

The second to last equality holds because  $X_i$  d-separates  $X_n$  from all earlier nodes. We conclude  $S(x_i) \geq \frac{3}{4}S(x_n) - \epsilon$  for all  $i \geq j$ . Since we have assumed  $S(x_i) \leq S(x_n)/4$  for all  $i < j$  we conclude that node  $j$  is the only one for which the anomaly scores shows a gap of at least  $1/2 - \epsilon$ , while the gap is smaller than  $1/4 + \epsilon$  for all others.

# C EXPERIMENTAL DETAILS AND FURTHER EXPERIMENTS

## C.1 Experimental details

To generate an SCM for the experiments in Section. 5 (see Fig. 1), we first uniformly sample between 10 and 20 root nodes (20% to 40% of the total nodes of the graph) and uniformly assign to each either a standard Gaussian, uniform, or mixture of Gaussians as its noise distribution. As a second step, we recursively sample non-root nodes. Non-root nodes need not be sink nodes. The number of parent nodes that each non-root node is conditioned on is randomly chosen following a distribution that assigns a lower probability to a higher number of parents. In total, the causal graph is composed of 50 nodes. The parametric forms of the structural equations are randomly assigned to be either a simple feed-forward neural network with a probability of 0.8 (to account for non-linear models) and a linear model. The feed-forward neural network has three layers (input layer, hidden layer, and output layer) where the hidden layer has a number of nodes chosen randomly between 2 and 100. All the parameters of the neural network are sampled from a uniform distribution between -5 and 5. For the linear model, we sample the coefficients of the linear model from a uniform distribution between -1 and 1 and set the intercept to 0. In both cases, we use additive Gaussian noise as the relation between the noise and the variables.

To generate data for the non-anomalous regime we sample the noise of each of the variables and propagate the noise forward using the previously sampled structural equations. As mentioned in the main text, to produce anomalous data we choose a root cause at random from the list of all nodes and a target node from the set of its descendants (including itself). Then we sample the noise of all variables and modify the noise of the root cause by adding  $x$  standard deviations, where  $x \in \{2, 2.1, \dots, 3\}$ , and propagate the noises through the SCM to obtain a realization of each variable. We repeat this process 100 times for each  $x$  value added to the standard deviation and consider the algorithm successful if its result coincides with the chosen root cause. **Computing Infrastructure.** All the experiments were run on a MacBook Pro with 16GB memory with an Apple M1 processor.

## C.2 Further experiments by varying the number of nodes in the graph

We also run experiments by fixing the number of standard deviations added ( $x$  in Section. 5) to 3 and varying the number of nodes in the SCM. Here, we have chosen the numbers  $\{20, 40, 60, 80, 100\}$ . We observe in Fig. 3 that the performance for Traversal, SMOOTH TRAVERSAL, and Counterfactual does not change much for different graph sizes, whereas the quality of TOCA and SCORE ORDERING decreases slightly for larger graph sizes. Circa, on the other hand, has worse performance for an intermediate number of nodes but the quality increases as the graph gets larger.

## C.3 How do the algorithms compare in terms of their practicality?

We should keep in mind that Counterfactual requires the SCM, while Traversal and SMOOTH TRAVERSAL require only the causal graph, this is a clear disadvantage of Counterfactual. In addition, Traversal needs

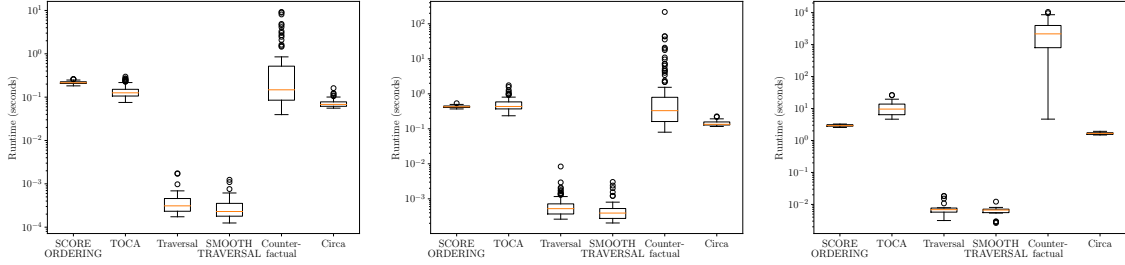


Figure 2: Runtimes of the algorithms for the experiment in Fig. 1; that is 50 nodes (left), an SCM with 100 nodes (center) and one with 1k nodes (right) (refer to the generation process above). The boxplots are produced using the default implementation in Matplotlib [48]. Note the log scale in the vertical axis.

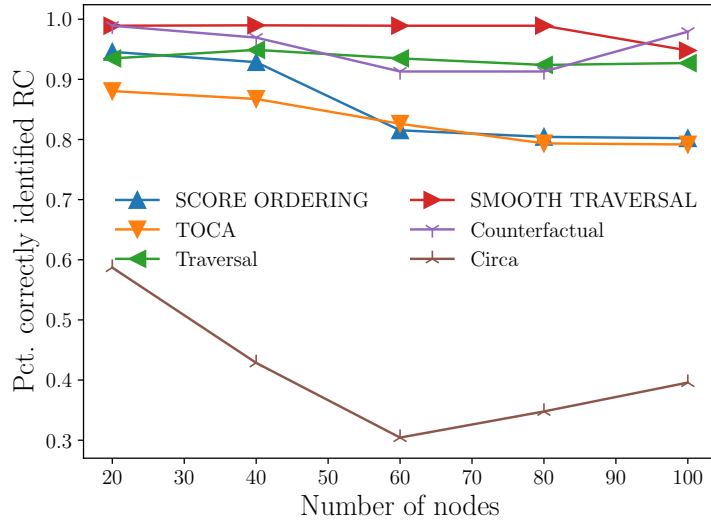


Figure 3: True positive rate of the compared algorithms in identifying the root cause with known structural assignments.

tuning the threshold parameter, while SMOOTH TRAVERSAL does not have a free parameter. Both SCORE ORDERING and TOCA have similar performance, but SCORE ORDERING does not even require information of the causal graph, whereas TOCA does. Nevertheless, it has the advantage over all others (except Counterfactual), that the inferred gap of log probabilities *witnesses a true causal contribution*, which is not the case for other methods since upstream anomalies may not be causally responsible for the target anomaly (as argued in Section 3). This way, TOCA is able to tell which node is a root cause in scenarios where there exists multiple root causes.

#### C.4 PetShop dataset

Hardt et al. [29] introduces a dataset from cloud computing, specifically designed for evaluating root cause analyses in microservice-based applications. The dataset is collected from a microservice application, and includes 68 injected performance issues, which increase latency and reduce availability throughout the system. Latency and availability are so-called ‘metrics’ of the microservice application, and measure the length of time it takes for a request to the service to be processed, and the fraction of the time a request returns an error, respectively. The dataset also encompasses three traffic scenarios, low, high and temporal. These correspond

to the amount and periodicity of user traffic to the application. This presents a challenging task due to high missingness, low sample sizes, and near-constant variables. Furthermore, the ground truth causal graph is only partially known as we must treat the edge inverted call graph as a proxy for the causal graph.

In addition to the approaches evaluated by Hardt et al. (see [29] for more details), which we have reproduced below, we evaluated our algorithms in both top-1 recall (Table. 1) and top-3 recall (Table. 2). In addition we included, as an additional baseline, the traversal algorithm as described in Section 5. This is added as although the evaluation already includes a ‘traversal’ algorithm implemented by Hardt et al., here called ‘petshop traversal’, their algorithm does not match the standard approach as described in [9, 27, 28]. Instead, ‘petshop traversal’ has been designed for use on the PetShop dataset, takes into account particular aspects of that data, and contrary to standard traversal algorithms, scores potential root causes according to anomalousness of whole paths of nodes from root cause to target node. ‘Petshop traversal’ should not, therefore, be treated as an ‘out-of-the-box’ baseline.

We observe that SMOOTH TRAVERSAL and SCORE ORDERING perform very well in top-1 and top-3 recall, often being the best performing algorithms, and clearly outperforming simple traversal. However, while SMOOTH TRAVERSAL always matches or exceeds the performance of simple traversal in top-1 recall, on latency issues it nonetheless tends to perform relatively poorly compared to SCORE ORDERING.

Note, however, the caveat that owing to the small sample size in the PetShop dataset, it is frequently the case that multiple anomalies (approx. 10 or more) receive the same highest score. The multiplicity of highest scores is due to the fact that for the issue at hand all these metrics were more extreme than ever sampled in the normal period. In this case, the root cause being in the top-1 means that it is among the variables receiving the highest score. This problem should become less severe for datasets where anomaly scorers are trained on a longer history. Since root cause analysis without any graphical information is a notoriously hard problem, returning short lists of potential root causes, even if they contain 10 or more candidates, can still result in a drastic reduction of the search space, and so is of vital use in real applications.

We, nonetheless, also report the top-1 (Table. 3) and top-3 (Table. 4) recall after randomly selecting among the nodes tied with the highest anomaly score. As expected, we observe an approx. 10x decrease in top-1 recall for traversal, SCORE ORDERING and SMOOTH TRAVERSAL, corresponding to selecting at random from among the approx. 10 candidate root causes with tied highest scores. Similar decreases are present in top-3 recalls for traversal and SCORE ORDERING whenever the true root cause is among those with the tied highest score. Note however that SMOOTH TRAVERSAL generally still has high top-3 recall even after random selection of the top-1 node, out performing both traversal and SCORE ORDERING.

		graph given			graph not given				this paper	
traffic scenario	metric	petshop traversal	circa	counter-factual	$\epsilon$ -diagnosis	rcd	correlation	traversal	SCORE ORDERING	SMOOTH TRAVERSAL
low	latency	0.57	0.36	0.36	0.00	0.07	0.43	0.14	<b>1.00</b>	0.14
low	availability	0.50	0.42	0.00	0.00	0.58	<b>0.75</b>	0.42	<b>0.75</b>	<b>0.75</b>
high	latency	0.57	0.50	0.57	0.00	0.00	0.64	0.14	<b>1.00</b>	0.14
high	availability	0.33	0.00	0.00	0.00	0.00	0.83	0.33	<b>1.00</b>	<b>1.00</b>
temporal	latency	<b>1.00</b>	0.75	0.38	0.12	0.25	0.62	0.25	0.75	0.25
temporal	availability	0.38	0.38	0.00	0.00	0.50	0.62	0.25	<b>1.00</b>	<b>1.00</b>

Table 1: Top-1\* recall, with ties. \*Multiple anomalies can receive the same, highest, anomaly score. The root cause being in the top-1 means that it is among the variables receiving the highest score.

		graph given			graph not given					<b>this paper</b>	
traffic scenario	metric	petshop traversal	circa	counter-factual	$\epsilon$ -diagnosis	rcd	correlation	traversal	SCORE ORDERING	SMOOTH TRAVERSAL	
low	latency	0.57	0.86	0.71	0.00	0.21	0.57	0.14	<b>1.00</b>	0.86	
low	availability	<b>1.00</b>	<b>1.00</b>	0.42	0.00	0.75	0.92	0.50	<b>1.00</b>	<b>1.00</b>	
high	latency	0.79	<b>1.00</b>	0.86	0.00	0.07	0.79	0.14	<b>1.00</b>	0.93	
high	availability	<b>1.00</b>	0.00	0.00	0.33	0.00	0.92	0.33	<b>1.00</b>	<b>1.00</b>	
temporal	latency	<b>1.00</b>	<b>1.00</b>	0.50	0.12	0.75	0.75	0.25	<b>1.00</b>	0.75	
temporal	availability	<b>1.00</b>	<b>1.00</b>	0.25	1.00	0.12	0.75	0.25	<b>1.00</b>	<b>1.00</b>	

Table 2: Top-3\* recall, with ties. \*Multiple anomalies can receive the same, highest, anomaly score. The root cause being in the top-3 means that it is among the variables ranked in the top three including all variables tied at the top.

				<b>this paper</b>	
traffic scenario	metric	traversal	SCORE ORDERING	SMOOTH TRAVERSAL	
low	latency	0.02	<b>0.10</b>		0.02
low	availability	0.06	<b>0.10</b>		<b>0.10</b>
high	latency	0.01	<b>0.06</b>		0.01
high	availability	0.03	0.06		<b>0.09</b>
temporal	latency	0.04	<b>0.10</b>		0.04
temporal	availability	0.04	0.13		<b>0.14</b>

Table 3: Top-1 recall, with random selection among ties.

				<b>this paper</b>	
traffic scenario	metric	traversal	SCORE ORDERING	SMOOTH TRAVERSAL	
low	latency	0.02	0.10		<b>0.73</b>
low	availability	0.10	<b>0.31</b>		<b>0.31</b>
high	latency	0.01	0.06		<b>0.80</b>
high	availability	0.03	0.06		<b>0.09</b>
temporal	latency	0.04	0.18		<b>0.54</b>
temporal	availability	0.04	0.13		<b>0.14</b>

Table 4: Top-3 recall, with random selection among ties